Construction and Building Materials 68 (2014) 102–109

Contents lists available at ScienceDirect

Construction and Building Materials

journal homepage: www.elsevier.com/locate/conbuildmat

The effect of glass powder on the microstructure of ultra high performance concrete

Vitoldas Vaitkevičius [a,*], Evaldas Šerelis [a], Harald Hilbig [b]

[a] Faculty of Civil Engineering and Architecture, Kaunas University of Technology, Studentų g. 48, LT-51367 Kaunas, Lithuania
[b] Centre of Building Materials, Technische Universität München, Munich, Germany

HIGHLIGHTS

- Dissolution of glass powder will make more dense structure of UHPC.
- Glass powder will additional increases compressive strength more than 30 MPa.
- Glass powder is a good contender for silica fume.
- Pozzolanic reaction is not primary beneficial property of glass powder.
- Purposed new hydration mechanism of the glass powder in Portland cement.

ARTICLE INFO

Article history:
Received 23 January 2014
Received in revised form 30 April 2014
Accepted 18 May 2014

Keywords:
Glass powder
Ultra-high performance concrete
Mercury intrusion porosimetry
XRD
^{29}Si MAS NMR

ABSTRACT

Glass powder prepared of various types of recycled bottles was used in ultra-high performance concrete (UHPC). Experimental investigation of glass powder as complete replacement for quartz powder and silica fume showed that UHPC with improved micro-structural and compressive strength properties can be prepared. Glass powder milled to micro-scale undergoes low pozzolanic reaction and acts as catalyst accelerating the dissolution of clinker phases and forms low basicity calcium silicate hydrate (C–S–H). These reactions give positive effect on mechanical and microstructural properties of UHPC. Microstructural investigation was made by mercury intrusion porosimetry (MIP), X-ray diffraction (XRD) analysis and by ^{29}Si MAS NMR analysis. Experimental results revealed that additional compressive strength of 40 MPa can be gained with combination of glass powder and silica fume.

1. Introduction

Glass is a solid material which generally consists of non-crystalline silica, sodium oxide, calcium oxide and other components [1–3]. The chemical composition mainly depends on the raw materials used and differs slightly for each glass type. The most common soda-lime glasses consist of $\geqslant$70% amorphous SiO_2, $\geqslant$12% Na_2O and $\geqslant$5% CaO [4–6]. Being amorphous and containing relatively large quantities of silicon, glass should be an excellent pozzolanic material for concrete industry. Thus when glass is finely grounded to powder, in theory, it could be used as partial cement replacement. However glass powder has very high amount of Na_2O which could initiate alkali–silica reaction. Therefore glass powder can be characterized by a few controversial facts: it has enough amorphous SiO_2 to be considered as pozzolanic material; available CaO can react with water and amorphous SiO_2 forming low basicity C–S–H. Glass also has a very high amount of Na_2O which is a source for alkali silica reaction. These truths are highly debated between various scientists; however it is not entirely clear how glass can affect microstructure of concrete with its high amount of alkalis. Most researchers denote three main factors which contribute to alkali silica reaction: sufficient amount of alkalis, reactive aggregate and sufficient amount of water [7–9]. However the following factors also have significant influence: water to cement ratio, permeability to moisture, solubility of alkalis, size of aggregates and type of concrete. The amount of Na_2O_{eq} is limited to 0.80% according to the EN 206:2013 standard [10]. Yet, there are plenty of cases where this limit is overstepped without deleterious effect on concrete. In order to understand how glass powder affects microstructure and properties of ultra-high performance concrete it is necessary to do a deeper research.

Corinaldesi et al. investigated the microstructure of mortars with 30–70% replacement of fine sand with particle size up to 100 μm varying w/c from 0.56 to 1.00. Compressive strength

* Corresponding author.
E-mail addresses: vitoltas.vaitkevicius@ktu.lt (V. Vaitkevičius), evaldas.serelis@ktu.lt (E. Šerelis), harald.hilbig@tum.de (H. Hilbig).

http://dx.doi.org/10.1016/j.conbuildmat.2014.05.101
0950-0618/

increased from 32 MPa to 60 MPa and this effect was attributed to the waste glass [11]. Zerbino et al. was working with mortars and concretes incorporating natural rice husk, varying the water to cement ratio from 0.44 to 0.56. He noticed swelling due to alkali silica reaction when $Na_2O_{eq} \geqslant 5.25$ kg/m^3. However that value mainly depends on capability of moisture transport in cement matrix [12]. Juengera and Ostertag in research used silica fume and sintered silica fume aggregate in concrete and noticed swelling in some specimens. This phenomenon was explained due to an inhomogeneous distribution of silica fume [13]. Saccani and Bignozzi investigated the solubility of various glasses in 1 N NaOH solution. He noticed that lead-silicate glass showed the highest dissolution rate, boro-silicate glass is less soluble comparing with lead-silicate glass and soda-lime glass is the most stable. Also it was observed that lime saturated water Ca^{2+} hinders the dissolution of glass irrespective of the chemical composition. The particles size of glass in the experiment varied from 0.075 mm to 2.00 mm [14]. Du and Tan investigated recycled green, brown and clear glass with particle size up to 0.75 μm and he noticed no deleterious expansions. Clear glass showed higher expansion, green glass showed about 3 times lower expansion than clear glass and brown glass showed about 9 time lower expansion than clear glass. The reduced expansion was attributed to Cr_2O_3 [15]. Wang and Huang used up to 30% of LCD glass with fineness modulus of 3.37 in self-consolidating concrete (W/C = 0.28) and noticed increased flexural strength from 4 MPa to 8 MPa and compressive strength from 40 MPa to 75 MPa. Also decreased permeability and increased resistance to sulphate attack were noticed [16]. Lin et al. used TFT and LCD waste glass with fineness of 370 m^2/kg (by Blaine) in his experiment and noticed a strong increase of C–S–H by ^{29}Si MAS NMR and a strong decrease of $Ca(OH)_2$ by Fourier transformation infrared spectroscopy [17]. Kou and Xing in experiment investigated properties of UHPC with W/B = 0.15 and used glass powder with particle size smaller than 0.0045 mm. He founded that replacement of cement by glass powder is very effective. However glass powder decreases early (7 days) compressive strength of UHPC. Reactivity of glass powder comparing to silica fume was is very low. In order to increase reactivity of glass powder thermal treatment should be applied [18]. Karakurt and Topçu activated ground granulated blast-furnace slag, natural zeolite and fly ashes with alkalis and noticed an improved microstructure of the concrete with an increased resistance to sulphate [19]. Shafaatian et al. noticed that fly ash acts as pH buffer which maintains pore solution's pH between 12.6 and 13.0. Also he found out that when glass powder is incorporated in mortars (W/C = 0.47) ASR gel occurs only between cracks of grounded glass particles. The particle size of the glass powder in the experiment varied from 150 μm to 4.75 mm [20]. Schwarz and Neithalath proposed a model for cement with fly ash and fine glass powder explaining pozzolanic properties of glass powders [21]. Amen noticed a drastically increasing compressive strength and decreasing permeability with porosity, when a cement paste has a water to cement ratio lower than 0.26 [22]. Idir et al. worked with glass powders of various sizes and noticed that the higher expansion can occur when the diameter of glass powder is $\geqslant$1000 μm. However its best pozzolanic performance is obtained when the particle size of the glass powder is between 10 μm and 20 μm [23]. Nassar and Soroushian worked with concrete (W/C varied from 0.38 to 0.50) using waste glass and noticed that glass with particle size of ~13 μm undergoes a pozzolanic reaction and improves the microstructure of a concrete. In addition a decrease of moisture sorption and chloride permeability was determined. The expansion of concrete specimens varied from 0.006% to 0.016% [24]. Ling et al. used recycled glass with fineness modulus of 3.33 and noticed improved structure and lower porosity of self-compacting concrete after exposure to thermal treatment. He attributed this to the pozzolanic reaction [25]. Ichikawa and Miura created a modified model for alkali silica reaction. The model explained a pessimum amount and a pessimum size effects. According to the model instead of alkali silica reaction pozzolanic reaction could occur, even when excessive amount of reactive aggregates are used [26]. Alkali silica gel could be found during the hydrolysis of reactive amorphous silica, which has similar properties as sodium silicate. Sodium silicate, also known as soluble glass in concrete industry also can sometimes be called water glass [27]. It seems that it is not entirely clear how glass improves or decreases the structure of concrete. However chemical composition, particle size and impurities of the glass powder have the biggest effect on a proper structure formation in concrete. Addition of other pozzolanic materials can suppress or even eliminate deleterious swelling. Although glass has a very high amount of amorphous silica it is not very reactive till it is finely grounded. Alkalis play an important role in cement hydrolysis process however the hydration mechanisms were not fully understood. It seems that when recycled glass is finely grounded in alkali environment it can dissolve and behave as water glass.

Shi experimented with various alkali activators (sodium and potassium hydroxides, silicates, carbonates and sulphates) and found that sodium silicate is the most effective activator [28,29]. Škvára proposed a theory and a model for a new amorphous material known as zeolite or geopolymer (N-A-S-H) which can form in a high alkaline environment when sufficient amount of Al is present [30]. Pacheco-Torgal et al. suggested a new mechanism explaining the geopolymer formation in alkaline solution [31]. Pacheco-Torgal et al. investigated the durability of alkali activated binders and noticed a very high stability in various environments and emphasizes that although sodium silicate is a promising activator however more research is needed [32,33]. García Lodeiro et al. researched C–S–H gel with different addition of alkali and aluminium. He determined by ^{29}Si and ^{27}Al NMR spectroscopy three-dimensional alkaline aluminosilicate gel cross-linking with two-dimensional C–S–H gel [34]. Buchwald et al. and Hilbig and Buchwald besides aluminosilicate network in alkali-activated metakaolin-slag blends founded stable C–S–H phases [35,36]. According to the literature there it is not entirely clear how glass powder affect the structure of UHPC. It looks as if coarse particle of glass ($\geqslant$0.20 mm) can initiate a deleterious swelling. However finely grounded glass powder up to 100 μm can act as a pozzolanic material or chemical activator. This phenomenon is not entirely clear. The main aim of this article is to find out how glass powder affects microstructure of UHPC, and by using mercury porosimetry, qualitative and quantitative XRD, by ^{29}Si MAS NMR and compressive test methods to explain the effect of glass powder on microstructure of UHPC. According to the literature review, properly recycled waste glass can not only increase durability and compressive strength of concrete but also can solve some major environmental, energy, and expenses problems by partial replacement of cement.

2. Used materials

2.1. Cement

Portland cement CEM I 52.5 R was used in the experiments. Main properties: paste of normal consistency – 28.5%; specific surface (by Blaine) – 4840 cm^2/kg; soundness (by Le Chatielier) – 1.0 mm; setting time (initial/final) – 110/210 min; compressive strength (after 2/28 days) – 32.3/63.1 MPa. Mineral composition: C_3S – 68.70; C_2S – 8.70; C_3A – 0.20; C_4AF – 15.90. The particle size distribution is shown in Fig. 1.

2.2. Silica fume

Silica fume, also known as microsilica (MS) or condensed silica fume is a by-product of the production of silicon metal or ferrosilicon alloys. Main properties: density – 2532 kg/m^3; bulk density – 400 kg/m^3; pH – 5.3. The particle size distribution is shown in Fig. 1.

2.3. Quartz powder

In the experiments quartz powder was used. Main properties: density 2671 kg/m^3; bulk density – 900 kg/m^3; average particle size – 18.12 μm; specific surface (by Blaine) – 4423 cm^2/g. The particle size distribution is shown in Fig. 1.

2.4. Glass powder

In the experiments glass powder was used. Main properties: density 2528 kg/m^3; average particle size – 25.80 μm; specific surface (by Blaine) – 3350 cm^2/g. The particle size distribution is shown in Fig. 2.

2.5. Quartz sand

In the experiments quartz sand was used. Main properties: fraction: 0/0.5; density 2650 kg/m^3; specific surface (by Blaine) – 91 cm^2/g.

2.6. Chemical admixture

In the experiments was used superplasticizer (SP) based on polycarboxylic ether (PCE) polymers. Main properties: appearance: dark brown liquid, specific gravity (20 °C) – 1.08 ± 0.02 g/cm^3; pH – 7.0 ± 1; viscosity – 128 ± 30 MPa; alkali content ⩽5.0%, chloride content ⩽0.1%.

3. Methods

3.1. Glass powder preparation

Various colours recycled bottles glass was used in the experiments. Recycled glasses with particle size up 5 cm were crushed with a jaw crusher to an average particle size of ~0.5 mm. Crushed glass particles were milled with a vibratory disc mill until a specific surface of 3350 cm^2/g was obtained. Main parameters of vibratory disc mill: cylindrical container diameter – 2171 mm; thickness of wall – 5.84 mm; height – 58.00 mm; mass – 6.246 kg. Materials were grinded with 3 smaller rings: (1) diameter – 184.60 mm, thickness – 14.50 mm, height – 47.55 mm, mass – 2.827 kg; (2) diameter – 134.05 mm, thickness – 14.50 mm, height – 45.50 mm, mass – 1.878 kg; (3) diameter 83.90 mm, height – 47.05, mass – 1.951 kg. Rotation speed is 750–940 rpm.

3.2. Specific surface and particle size distribution

The specific surface was measured with Blaine instrument according to the EN 196-6:2010 standard [37]. The particle size distribution was measured with a "Mastersize 2000" instrument produced by Malvern Instruments Ltd. Optimal particle size distribution was calculated according to Yu et al. and Nguyen et al. [38,39].

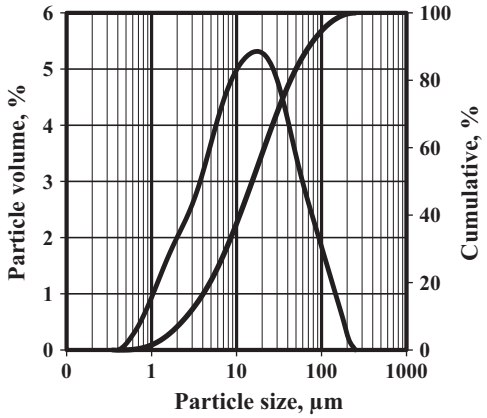

Fig. 2. Particle size distribution of glass powder.

3.3. Mixing, sample preparation and curing

Fresh concrete mixes were prepared with an "*EIRICH R02*" mixer. The mixtures were prepared from dry aggregates. Cement and aggregates were dosed by weight, water and chemical admixtures were added by volume (Tables 1 and 2). Cylinders (d = 50 mm, h = 50 mm) were formed for the research to determine concrete properties. Homogeneous mixes were cast in moulds and kept for 24 h at 20 °C/95 RH (without compaction). After 24 h thermal treatment (1 + 18 + 3) was applied and rest of the time till age of 28 days specimens were kept under water at 20 °C.

3.4. Mercury intrusion porosimetry (MIP) test

At the age of 28 days, cylinders (d = 50 mm, h = 50 mm) of each composition were broken into small fragments and placed in isopropanol. Later these fragments were dried at 40 °C to remove all free water. These dried fragments were stored in sealed containers for MIP tests. The pressure was applied from 0 MPa to 450 MPa. A Constant contact angle of 140° and a constant surface tension of mercury of 480 mN/m were assumed for the pore size calculation.

3.5. X-ray diffraction (XRD) analysis

The hardened cement pastes were used for XRD analysis. The XRD measurements were performed with a XRD 3003 TT diffractometer of GE Sensing & Inspection Technologies GmbH with θ–θ configuration und CuKα radiation (λ = 1.54 Å). The angular range was from 5 to 70° 2 Theta with a step width of 0.02° and a

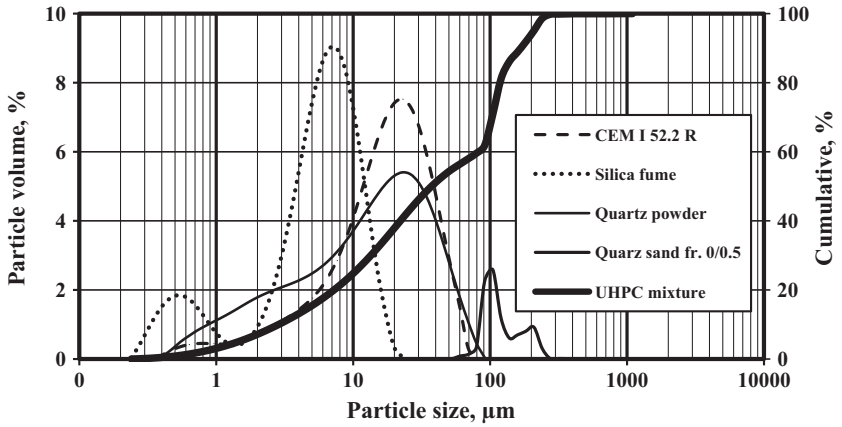

Fig. 1. Particle size distribution of Portland cement, silica fume, quartz powder and 0/0.5 fr. quarts sand.

Table 1
Chemical compositions of Portland cement, silica fume and glass powder.

Components	Quantity, %		
	CEM I 52.5 R	Silica fume	Glass powder
SiO_2	21.10	97.60	72.76
TiO_2	0.22	0.00	0.04
Al_2O_3	3.42	0.80	1.67
Fe_2O_3	5.23	0.05	0.79
MnO	0.05	0.00	0.02
MgO	0.79	0.13	2.09
CaO	66.40	0.37	9.74
SO_3	1.93	0.08	0.10
Na_2O	0.19	0.00	12.56
K_2O	0.38	0.19	0.76
P_2O_5	0.28	0.00	0.02
Na_2O_{ekv}	0.44	0.13	13.06
Loss of ignition	0.60	0.60	1.00

measuring time of 6 s/step. For XRD quantitative phase analysis using the Rietveld refinement the samples were mixed with 20 wt.% ZnO (a standard material widely used in XRD analysis) as an internal standard and stored in argon atmosphere until measurement. This permits the estimation of the amount of non-crystalline phases by the Rietveld fitting procedure.

3.6. Nuclear magnetic resonance (NMR) analysis

Solid state NMR was performed with a Brucker Avance 300 spectrometer (magnetic field strength 7.0455 T, resonance frequency of ^{29}Si is 59.63 MHz). To measure the ^{29}Si MAS NMR spectra, the samples were packed in 7 mm zirconia rotors and spun at 5 kHz at an angle of 54°44́ (MAS). The chemical shifts were recorded relative to external tetramethylsilane (TMS). The single pulse technique was applied with a pulse width of 6 μs. Owing to the slow relaxation of the silica fume a repetition time of 45 s was chosen and a typical number of scans was 2000. Thirty Hertz line broadening was applied to all spectra prior to deconvolution. The signal patterns of the spectra were deconvoluted with the Bruker WINNMR software. The interpretation of the ^{29}Si NMR spectra was performed according to Schachinger and Harald [40]. Because of the high Fe-content of the cement it was necessary to include the first spinning side bands. To avoid additional signals all mixtures for the NMR investigations were prepared without quartz.

3.7. Compressive strength

Compressive strength was performed after 28 days according to EN 12390-4 standard [41]. Compressive strength was obtained from 6 cylinders (d = 50 mm; h = 50 mm) as average value.

4. Results

According to the methods described before, four compositions of UHPC with different amount of glass powder were created (Table 2). QP/GP0 is as reference composition, QP/GP100 when quartz powder was substituted by 100% of glass powder. In QP/GP100SF/GP100 quartz powder and silica fume were substituted by 100% of glass powder and in SF/GP100 silica fume was substituted by 100% of glass powder. For investigation following techniques were applied: mercury intrusion porosimetry (MIP), qualitative and quantitative XRD analysis, NMR and compressive strength tests methods.

4.1. Pore size distribution

The compositions with glass powder (QP/GP100 and QP/GP100SF/GP100) exhibited a significantly lower measured porosity and had not macroporosity (Figs. 3 and 4). The composition without glass powder (QP/GP0) had a continuous pore size distribution up to 700 μm while the compositions with glass powder (QP/GP100 and QP/GP100SF/GP100) had up to 70 μm. Reduced macroporosity significantly affects mechanical properties of UHPC. The most reduced porosity was observed in the composition with silica fume and glass powder (QP/GP100). Another interesting fact was observed: all compositions had a higher concentration of pores at nanoscale $\leqslant$0.1. These types of pores do not influence mechanical properties but mostly affects the shrinkage and creep of concrete. XRD analysis was applied in order to find out why UHPC with glass powder showed a lowered pore size distribution.

4.2. XRD analysis

Qualitative and quantitative XRD analysis was applied in order to obtain information on the phase compositions of the cement pastes. Fig. 5 illustrates the XRD patterns of the four hardened cement pastes with different amount of glass powder. CH phase was found at 17.9°, 33.9°, 46.8°, 50.2° and 53.8°. Evidently the crystalline phase of CH was decreased with an increase of glass powder. C_2S and C_3S phases were found at 29.3°, 29.7°, 31.9°, 38.3°, 41.3°, 45.3°, 49.4°, 51.2° and 59.6°. It was noticed, that when amount of glass powder increases, intensities of C_2S and C_3S tends to decrease. Decreased C_2S and C_3S peaks are probably related with a better solubility of the clinker phase. Pozzolanic reaction by portlandite with silica fume and glass powder, probably, had the biggest influence on decreased intensities of CH peaks.

The results of X-ray diffraction measurements were analysed using the Rietveld method (Table 3 and Fig. 6). The experiment results revealed that the clinker phases with glass powder reacted more intensively comparing with reference mixture (QP/GP0). Glass powder and silica fume may react with portlandite to form additional C–S–H phases. However glass powder drastically increased solubility of clinker phases probably due to high amount of alkalis. The best performance showed composition (QP/GP100) when 100% of quartz powder was substituted by glass powder: $C_2S + C_3S$ decreased about for 12% from 45.1% to 33.1%; C_2S decreased about for 9% from 34.2% to 25.4; C_3S decreased about for 3% from 10.9% to 7.7%; C_4F decreased about for 2.5% from 7.0% to 4.5%; portlandite decreased about for 4% from 7.0% to 3.8%. The best clinker solubility performance was obtained with composition (QP/GP100SF/GP100) when 100% of quartz powder and 100% of silica fume were substituted by glass powder: $C_2S + C_3S$ decreased about 16% from 45.1% to 29.18%. Even when 100% of silica fumes were substituted by glass powder, the solubility of clinker

Table 2
Compositions of Ultra high performance concrete.

Composition	Water, l	Cement, kg/m^3	W/C	Microfiller, kg/m^3			Quartz sand 0/0.5, kg/m^3	SP, l
				Silica fume	Quartz powder	Glass powder		
QP/GP0	186	735	0.25	99	412	–	962	30.65
QP/GP100					–	391		
QP/GP100SF/GP100				–	–	489		
SF/GP100				–	412	99		

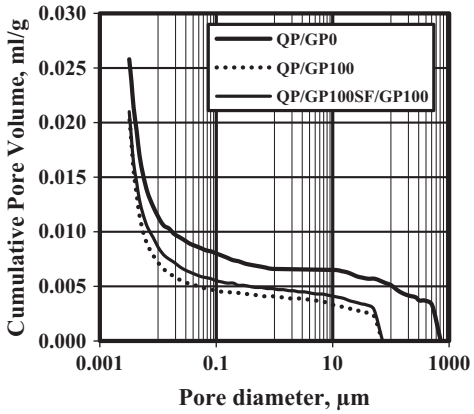

Fig. 3. MIP pore diameter versus cumulative pore volume.

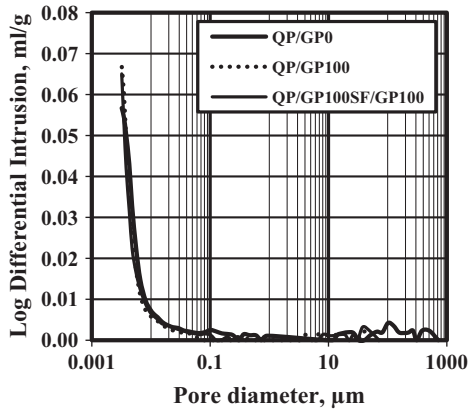

Fig. 4. MIP pore diameter versus log differential intrusion.

drastically increased: $C_2S + C_3S$ decreased about for 13% from 45.1% to 32.3. However, glass powder is not so effective pozzolanic material as silica fume and leaves high amounts of unreacted portlandite (Table 3).

Portlandite makes an inhomogeneous microstructure, which has a negative effect for the compressive strength of UHPC. Experimental results revealed that the glass powder can bind about 5 times less portlandite comparing with silica fume. However, the particle size distribution, the fineness of the glass powder and the pH value of the pore solution also has very important role. Another interesting fact was noticed, that cement pastes with glass powder had an increased amount of amorphous phase (Fig. 6). Although increased amount of amorphous phase could be attributed to increased amount of C–S–H phases, however to this phase also could be attributed unreacted silica fume and glass powder. In order to clarify the experimental data another method was applied.

4.3. ^{29}Si MAS NMR analysis and compressive strength

Peak assignments were made using the standard Q^n nomenclature [42]. Because of the overlapping signals following regime for deconvolution was applied: First the spectra of the pure powder and the mixture QP/GP0 having less overlap were deconvoluted. The signal of the glass powder could be fitted with to curves, contributing to Q^3 and Q^4 in a ratio of about 4–1.The spectrum of QP/GP0 delivered parameter for the unhydrated cement phases C_3S and C_2S, the C–S–H and the remaining silica fume (Fig. 8). The resulting peak positions and widths were used as fixed values for the deconvolution of the other more overlapping spectra. ^{29}Si MAS NMR spectra of the different mixtures are shown in Fig. 7. The resulting distributions of the silicate phases and the calculated values before hydration are shown in Table 4. Calculated hydration degrees of the components are shown in Table 5.

As expected the silicate phases of the glass powder showed more or less no puzzolanic reaction after that short time of hydration. Nevertheless glass powder increases solubility of Portland cement phases confirming XRD analysis data. The composition when 100% of quartz powder were substituted by glass powder had about 4% increased amount of reacted cement; the composition when 100% of quartz powder and 100% of silica fume were substituted by glass powder had about 23% increased amount of reacted cement; even composition when 100% of silica fume was substituted by glass powder had about 18% increased amount of reacted cement. The accelerating effect is not correlated with the amount of the glass powder. The highest hydration degrees are determined when silica fume is substituted. However all composition had mean C–S–H chain length of ~5.00.

The highest compressive strength was obtained in composition (QP/GP100) with silica fume and where 100% of quartz powder was substituted by glass powder. The compressive strength increased about 40 MPa from 182 MPa to 221 MPa (Fig. 9). When 100% of quartz powder and 100% of silica fume was substituted by glass powder (QP/GP100SF/GP100) compressive strength remained almost the same. When 100% of silica fume was substituted by glass powder (SF/GP100) the compressive strength started decreasing and confirmed the assumption that glass powder is not as good pozzolanic material as silica fume.

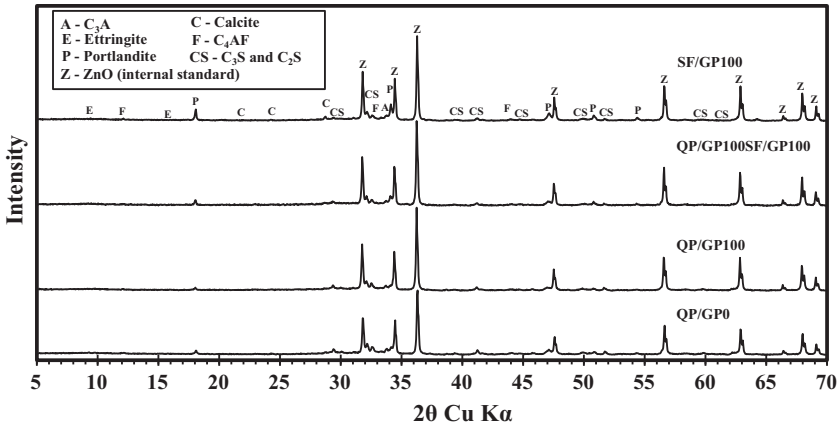

Fig. 5. XRD patterns of hardened cement pastes with different amount of glass powder.

Table 3
Mineralogical composition of the binder for UHPC with different amount of glass powder.

Phases	QP/GP0		QP/GP100		QP/GP100SF/GP100		SF/GP100	
	wt.%	sd	wt.%	sd	wt.%	sd	wt.%	sd
Amorphous	38.0	3.9	56.4	3.0	58.9	2.8	50.2	2.6
C_2S	34.2	3.9	25.4	3.3	24.1	2.7	27.2	2.5
C_3S	10.9	1.1	7.7	0.8	5.1	0.9	5.1	0.8
C_4AF	7.0	1.1	4.5	0.8	3.9	0.9	5.4	0.8
Calcite	2.8	0.6	2.2	0.4	2.0	0.5	1.6	0.5
Portlandite	7.0	0.6	3.8	0.5	6.1	0.7	10.5	0.7
Total	100.0	–	100.0	–	100.0	–	100.0	–
$C_2S + C_3S$	45.1	–	33.1	–	29.18	–	32.3	–

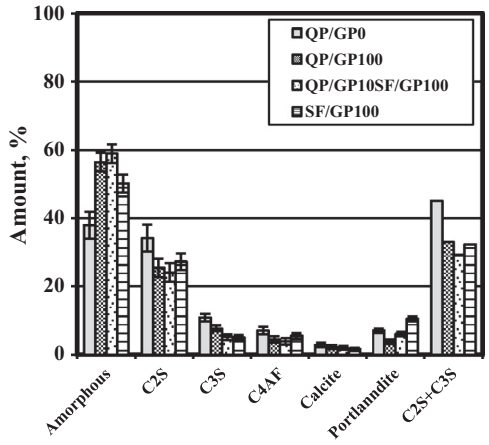

Fig. 6. Mineralogical composition of the binder with different amount of glass powder.

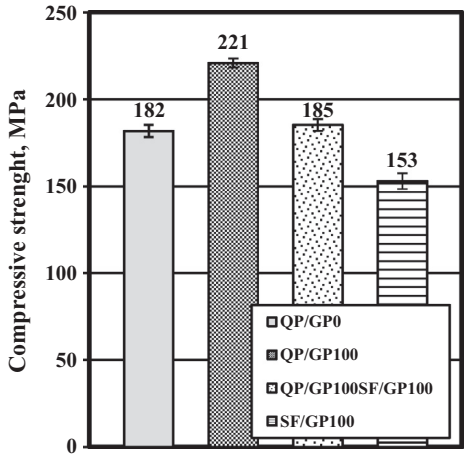

Fig. 7. Compressive strength of UHPC with different amount of glass powder.

Extensive experiment was carried out to create optimal composition of UHPC. The research revealed that glass powder can be successfully incorporated in UHPC without any loss of compressive strength. Milled glass can certainly substitute silica fume, quartz powder and even reduce amount of Portland cement. Thus price of UHPC can be drastically reduced. Ternary system of cement, glass powder and silica fume has positive effect for maximal compressive strength (QP/GP100). Compressive strength can be obtained up to 220 MPa. However maximal economic benefit can be achieved when glass powder is used instead of silica fume and quartz powder (QP/GP100SF/GP100). The results of the experiment revealed, that all compositions has enormous amount of

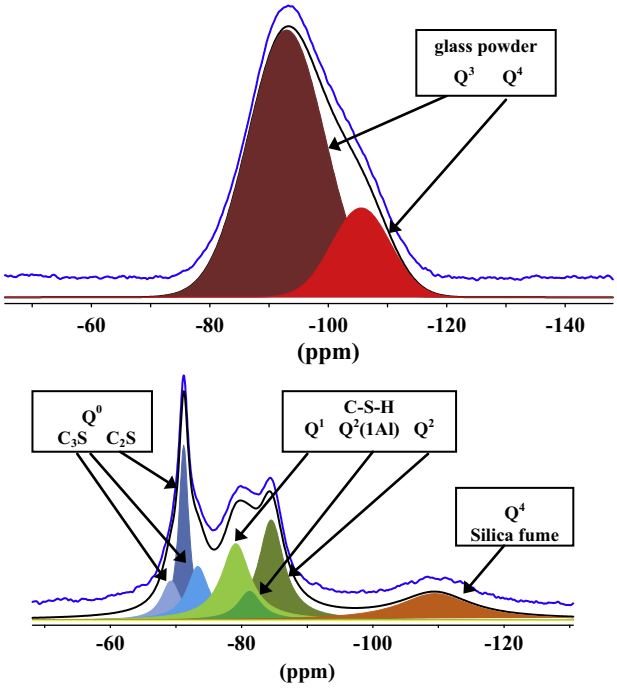

Fig. 8. ^{29}Si MAS NMR spectra with interpretation of the glass powder (up) and QP/GP0 (below).

unreacted cement. It can be still reduced, economic benefit can be increased even further, however additional research is needed.

5. Discussion

The gain in mechanical strength of UHPC appears to be the outcome of glass powder. Glass powder acts more as chemical activator than pozzolanic material however possess both characteristics. In the early hydration stage glass powder acts as inert material. In some cases glass powder can reduce water amount for normal consistency mixture and in other cases it acts in opposite way. This probably depends on particle size distribution, specific surface and defects in the glass powder. When pore solution reaches pH $\geqslant$ 13.0 dissolution rate of glass powder rapidly increases. Dissolution of glass powder is endothermic process, so heat treatment increases dissolution rate. Dissolution of glass releases high amount of alkalis which acts as a catalyst for the decomposition of Portland cement, silica fumes and glass powder. In high alkaline environment glass powder undergoes alkali silica reaction. If the particle size of glass powder is small enough – 0.25 mm, formed alkali silica gel does not have negative expansion effect and could be treated as sodium silicate known as water glass.

Table 4
Silicate distribution in the phases of cement pastes with different amount of glass powder (in brackets values before hydration).

Composition	Content, mol% Si			
	Unhydrated cement	Unhydrated silica fume	Unhydrated glass powder	C–S–H
QP/GP0	33 (62)	14 (39)	–	53 (0)
QP/GP100	14 (29)	6 (18)	53 (53)	26 (0)
QP/GP100SF/GP100	9 (30)	–	66 (69)	25 (0)
SF/GP100	24 (69)	–	32 (32)	45 (0)

Table 5
Hydration degrees of the silicate phases of admixtures.

Composition	Hydration degree, mol% Si			C–S–H mol% Si	Mean C–S–H chain length	Compressive strength, MPa
	Cement	Silica fume	Glass powder			
QP/GP0	47	64	–	53	4.6	182
QP/GP100	51	66	0	26	4.4	221
QP/GP100SF/GP100	70	–	5	25	5.2	185
SF/GP100	65	–	0	45	4.6	153

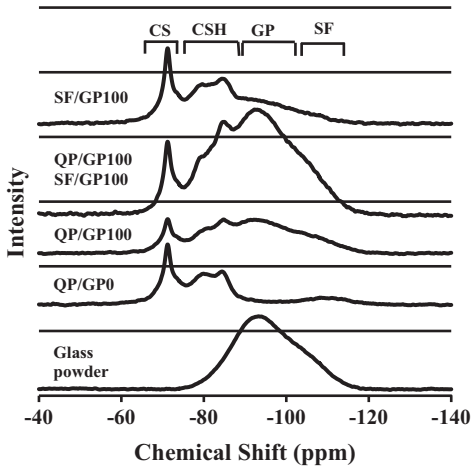

Fig. 9. ^{29}Si MAS NMR spectra of the binder with different amount of glass powder.

Further hydration process is influenced by sodium content and the silica modulus (M_s). The higher Na_2O and M_s the higher hydration level of cement will be obtained. However optimal values depend on type of the concrete, water to cement ratio, parameters of thermal treatment and etc. Water glass homogeneously distributed in all composition drastically decreases porosity of UHPC which is beneficial for mechanical and durability properties. Increased solubility of Portland cement also increase amount of portlandite. Amorphous silica in glass powder may react with CH and forms low basicity C–S–H in a later stage of hydration. The alkalies will be incorporated into new formed hydration phases mostly in low basicity C–S–H. Thus the microstructure of concrete and compressive strength could be increased significantly and UHPC with superior mechanical properties prepared.

6. Conclusions

Glass powder, when milled to about the particle size of cement (micro-scale), undergoes timely beneficial reaction with cement phases, forming calcium silicate hydrate (C–S–H) which benefits the structure and properties of ultra-high performance concrete. Based on the results of the study, the following conclusions can be drawn:

(1) Due to the positive effect of an alkali silica reaction in the compositions with glass powder macroporosity was eliminated and a largest pores at micro-scale ($\leqslant$70 μm) observed. All compositions of UHPC had the highest concentration of pores at Nano-scale ($\leqslant$0.1 μm).
(2) Quantitative and qualitative XRD analysis revealed that glass powder increases dissolution rate of Portland cement, thus hydration process is accelerated. Glass powder does not possess as good pozzolanic properties as silica fume. Silica fume consumes CH almost 5 times more, than glass powder.
(3) ^{29}Si MAS NMR analysis confirmed the results of XRD analysis, that glass powder increases dissolution rate of Portland cement. Highest amount of reacted cement (70%) was observed in the composition where 100% of silica fume and 100% of quartz powder were substituted by glass powder. The lowest amount of reacted cement (44%) was observed in the reference composition without glass powder. Despite of the amount of glass powder used in mixtures but in all composition reacted amount of glass powder was very low. The raising effect on the cement hydration is attributed to fast soluble alkali from the surface.
(4) Worst performance and compressive strength (153 MPa) was observed in the composition when 100% of silica fume was substituted by glass powder. Best performance and compressive strength (221 MPa) was observed in composition with combination of silica fume and glass powder.

Acknowledgment

This work has been supported by the European Social Fund within the project "Development and application of innovative research methods and solutions for traffic structures, vehicles and their flows", project code VP1-3.1-ŠMM-08-K-01-020.

References

[1] Khatib JM, Negim EM, Sohl HS, Chileshe N. Glass powder utilisation in concrete production. Eur J Appl Sci 2012;4(4):173–6. http://dx.doi.org/10.5829/idosi.ejas.2012.4.4.1102.
[2] Madandoust Rahmat, Ghavidel Reza. Mechanical properties of concrete containing waste glass powder and rice husk ash. Biosyst Eng 2013;116(2):113–9. http://dx.doi.org/10.1016/j.biosystemseng.2013.07.006.
[3] Mageswari M, Vidivelli B. The use of sheet glass powder as fine aggregate replacement in concrete. Open Civil Eng J 2010;4:65–71. http://dx.doi.org/10.2174/1874149501004010065.

[4] Balandis A, Vaickelionis G. Stiklo defektų susijusių su stiklo duženų naudojimu įkrovoje, analyze. ISSN 1392-1231. CHEMINĖ TECHNOLOGIJA. 2012. Nr. 1(59) http://dx.doi.org/10.5755/j01.ct.59.1.1526.
[5] Zanotto Edgar Dutra. Surface crystallization kinetics in soda-lime-silica glases. J Non-Cryst Solids 1991;129:183–90. DOI: no.
[6] Pigeonneau F, Muller S. The impact of iron content in oxidation front in soda-lime silicate glasses: an experimental and comparative study. J Non-Cryst Solids 2013;380:86–94. http://dx.doi.org/10.1016/j.jnoncrysol.2013.09.003.
[7] Venkatanarayanan Harish Kizhakkumodom, Rangaraju Prasada Rao. Decoupling the effects of chemical composition and fineness of fly ash in mitigating alkali–silica reaction". Cement Concr Compos 2013;43:54–68. http://dx.doi.org/10.1016/j.cemconcomp.2013.06.009.
[8] Pignatelli Rossella, Comi Claudia, Monteiro Paulo JM. A coupled mechanical and chemical damage model for concrete affected by alkali–silica reaction". Cem Concr Res 2013;53:196–210. http://dx.doi.org/10.1016/j.cemconres.2013.06.011.
[9] Moon Juhyuk, Speziale Sergio, Meral Cagla, Kalkan Bora, Clark Simon M, Monteiro Paulo JM. Determination of the elastic properties of amorphous materials: case study of alkali–silica reaction gel". Cem Concr Res 2013;54:55–60. http://dx.doi.org/10.1016/j.cemconres.2013.08.012.
[10] EN 206:2013 Concrete. Specification, performance, production and conformity.
[11] Corinaldesi V, Gnappi G, Moriconi G, Montenero A. Reuse of ground waste glass as aggregate for mortars. Waste Manage (Oxford) 2005;25:197–201. http://dx.doi.org/10.1016/j.wasman.2004.12.009.
[12] Zerbino R, Giaccio G, Batic OR, Isaia GC. Alkali–silica reaction in mortars and concretes incorporating natural rice husk ash. Constr Build Mater 2012;36:796–806. http://dx.doi.org/10.1016/j.conbuildmat.2012.04.049.
[13] Juengera MCG, Ostertag CP. Alkali–silica reactivity of large silica fume-derived particles. Cem Concr Res 2004;34:1389–402. http://dx.doi.org/10.1016/j.cemconres.2004.01.001.
[14] Saccani Andrea, Bignozzi Maria Chiara. ASR expansion behavior of recycled glass fine aggregates in concrete. Cem Concr Res 2010;40:531–6. http://dx.doi.org/10.1016/j.cemconres.2009.09.003.
[15] Du Hongjian, Tan Kiang Hwee. Use of waste glass as sand in mortar: Part II – Alkali–silica reaction and mitigation methods. Cement Concr Compos 2013;35:118–26. http://dx.doi.org/10.1016/j.cemconcomp.2012.08.029.
[16] Wang Her-Yung, Huang Wen-Liang. Durability of self-consolidating concrete using waste LCD glass. Constr Build Mater 2010;24:1008–13. http://dx.doi.org/10.1016/j.conbuildmat.2009.11.018.
[17] Lin Kae-Long, Wang Nian-Fu, Shie Je-Lueng, Leec Tzen-Chin, Lee Chau. Elucidating the hydration properties of paste containing thin film transistor liquid crystal display waste glass. J Hazard Mater 2008;159:471–5. http://dx.doi.org/10.1016/j.jhazmat.2008.02.044.
[18] Kou Shi Cong, Xing Feng. The effect of recycled glass powder and reject fly ash on the mechanical properties of fibre-reinforced ultrahigh performance concrete. Adv Mater Sci Eng 2012; Article ID 263243: 8 p http://dx.doi.org/10.1155/2012/263243.
[19] Karakurt Cenk, Topçu Ilker Bekir. Effect of blended cements produced with natural zeolite and industrial by-products on alkali–silica reaction and sulfate resistance of concrete. Constr Build Mater 2011;25:1789–95. http://dx.doi.org/10.1016/j.conbuildmat.2010.11.087.
[20] Shafaatian Seyed MH, Akhavan Alireza, Maraghechi Hamed, Rajabipour Farshad. Howdoes fly ash mitigate alkali–silica reaction (ASR) in accelerated mortar bar test (ASTM C1567)? Cement Concr Compos 2013;37:143–53. http://dx.doi.org/10.1016/j.cemconcomp.2012.11.004.
[21] Schwarz Nathan, Neithalath Narayanan. Influence of a fine glass powder on cement hydration: comparison to fly ash and modeling the degree of hydration. Cem Concr Res 2008;38:429–36. http://dx.doi.org/10.1016/j.cemconres.2007.12.001.
[22] Dillshad KH Amen. Degree of hydration and strength development of low water-to-cement ratios in silica fume cement system. Int J Civ Environ Eng IJCEE-IJENS 11(05), 2011, (DOIL no).
[23] Idir R, Cyr M, Tagnit-Hamou A. Use of waste glass as powder and aggregate in cement-based materials. In: SBEIDCO – 1st international conference on sustainable built environement infrastructures in developing countries ENSET Oran (Algeria); October 12–14, 2009. p. 109–16. http://dx.doi.org/10.1016/j.conbuildmat.2009.12.030.
[24] Nassar Roz-Ud-Din, Soroushian Parviz. Strength and durability of recycled aggregate concrete containing milled glass as partial replacement for cement. Constr Build Mater 2012;29:368–77. http://dx.doi.org/10.1016/j.conbuildmat.2011.10.061.
[25] Ling Tung-Chai, Poon Chi-Sun, Kou Shi-Cong. Influence of recycled glass content and curing conditions on the properties of self-compacting concrete after exposure to elevated temperatures. Cement Concr Compos 2012;34:265–72. http://dx.doi.org/10.1016/j.cemconcomp.2011.08.010.
[26] Ichikawa Tsuneki, Miura Masazumi. Modified model of alkali–silica reaction. Cem Concr Res 2007;37:1291–7. http://dx.doi.org/10.1016/j.cemconres.2007.06.008.
[27] Ichikawa Tsuneki. Alkali–silica reaction, pessimum effects and pozzolanic effect. Cem Concr Res 2009;39:716–26. http://dx.doi.org/10.1016/j.cemconres.2009.06.004.
[28] Shi Caijun, Zheng Keren. A review on the use of waste glasses in the production of cement and concrete. Resour Conserv Recycl 2007;52:234–47. http://dx.doi.org/10.1016/j.resconrec.2007.01.013.
[29] Shi Caijun. Strength, pore structure and permeability of alkali-activated slag mortars. Cem Concr Res 1996;26(12):1789–99. http://dx.doi.org/10.1016/S0008-8846(96)00174-3.
[30] Škvára František. Alkali activated materials or geopolymers. Ceramics – Silikáty 2007;51(3):173–7. DOI:NO.
[31] Pacheco-Torgal Fernando, Castro-Gomes Joa~o, Jalali Said. Alkali-activated binders: a review Part 1. Historical background, terminology, reaction mechanisms and hydration products. Constr Build Mater 2008;22:1305–14. http://dx.doi.org/10.1016/j.conbuildmat.2007.10.015.
[32] Pacheco-Torgal Fernando, Castro-Gomes Joao, Jalali Said. Alkali-activated binders: a review. Part 2. About materials and binders manufacture. Constr Buil 2008;22(7):1315–22. http://dx.doi.org/10.1016/j.conbuildmat.2007.03.019.
[33] Pacheco-Torgal F, Abdollahnejad Z, Camões AF, Jamshidi M, Ding Y. Durability of alkali-activated binders: a clear advantage over Portland cement or an unproven issue? Constr Build Mater 2012;30:400–5. http://dx.doi.org/10.1016/j.conbuildmat.2011.12.017.
[34] García Lodeiro I, Fernández-Jimenez A, Palomo A, Macphee DE. Effect on fresh C–S–H gels of the simultaneous addition of alkali and aluminium. Cem Concr Res 2010;40:27–32. http://dx.doi.org/10.1016/j.cemconres.2009.08.004.
[35] Buchwald A, Hilbig H, Kaps Ch. Alkali-activated metakaolin-slag blends – performance and structure in dependence of their composition. J Mat Sci 2007;42:3024–32. http://dx.doi.org/10.1007/s10853-006-0525-6.
[36] Hilbig H, Buchwald A. The effect of activator concentration on reaction degree and structure of alkali-activated ground granulated blast furnace slag. J Mat Sci 2006;41:6488–91. http://dx.doi.org/10.1007/s10853-006-0755-7.
[37] EN 196-6:2010. Methods of testing cement – Part 6: determination of fineness.
[38] Yu R, Spiesz P, Brouwers HJH. Mix design and properties assessment of Ultra-High Performance Fibre Reinforced Concrete (UHPFRC). Cem Concr Res 2014;56:29–39. http://dx.doi.org/10.1016/j.cemconres.2013.11.002.
[39] Nguyen Duy Liem, Ryu Gum Sung, Koh Kyung Taek, Kim Dong Joo. Size and geometry dependent tensile behavior of ultra-high-performance fiber-reinforced concrete. Composites 2014;58:279–92. http://dx.doi.org/10.1016/j.compositesb.2013.10.072.
[40] Schachinger Ingo, Hilbig Harald, Stengel Thorsten. Effect of curing temperature at an early age on the long-term strength development of UHPC. In: Proceedings of the second international symposium on ultra high performance concrete, No.10. Kassel, Germany; March 05–07, 2008. p. 205–12 (DOI: no).
[41] EN 12390-4:2000. Testing hardened concrete – Part 4: Compressive strength – specification for testing machines.
[42] Engelhardt G, Michel D. High-resolution solid-state NMR of silicates and zeolites. Chichester: John Wiley and Son; 1987. http://dx.doi.org/10.1017/S0016756800006361.